

HIGH PERFORMANCE POWER DIODES ON SILICON CARBIDE AND DIAMOND

Gheorghe BREZEANU

University “POLITEHNICA” Bucharest, Splaiul Independentei 313, 060032, Romania
E-mail: Gheorghe.Brezeanu@dce.pub.ro

Silicon Carbide and diamond Schottky barrier diodes (SBD) with an original and high efficiency termination are presented. The influences of termination parameters on the diodes electrical performance are investigated for both punch-through (PT) and non punch-through (nPT) structures by simulations. Design guidelines, based on simple analytical expressions, for ideal SBDs are included. Electrical forward and reverse characteristics, measured on SiC and diamond devices produced for the first time in Romania are also offered.

Key words: Silicon carbide, Diamond, Schottky diodes, Oxide ramp termination, Breakdown voltage, Termination efficiency

1. INTRODUCTION

In the last decades, significant advances in Silicon-based power devices and systems had a considerable industrial impact. Hence, they are now used in a wide range of power electronic applications such as lamp ballast, motor control, medical electronics, and high frequency power supplies [1], [2]. However, Si power devices are approaching their theoretical limits and are not able to meet the continuous demand for higher current (over 5 kA), higher voltage blocking capacity (over 20 kV), higher operating temperature (over 200⁰C) and improvements in terms of efficiency, size and weight [2]. These suggest that a new generation of power devices based on wide band gap semiconductors is needed to exceed these limitations.

Wide band gap semiconductors such as diamond (Dia) , silicon carbide (SiC), and gallium nitride (GaN) are the promising materials for new power devices. Diamond and SiC have been specifically known for some time to be excellent semiconductors for high temperature and high-speed electronics [1-10]. These materials have exhibited very high microwave conductivity and are known to be less susceptible to radiation effects.

This paper is focused on the investigation of the power Schottky barrier diodes (SBD) on SiC and synthetic diamond, produced for the first time in Romania [11-19]. Firstly, some simple algorithms to design SiC and Dia SBDs are described. Based on analytical equations, large capabilities of these devices for forward current and blocking voltage will be demonstrated. An efficient field plate termination for SiC and diamond devices is proposed experimented and tested [11-14]. Extensive simulation results, for different termination parameters and for punch-through and non punch-through structures are presented [18]. Experimental data measured on SiC and diamond SBDs prove the simulations.

2. SIC AND DIAMOND PARAMETERS

In Table 1 are presented some fundamental parameters of the diamond towards its possible applications. Table 2 compares power related parameters of wide-gap semiconductors and its impact for power and high frequency applications. As observed in this table, diamond has the highest breakdown

electric field, thermal conductivity, electron saturation velocity, and carrier mobilities. In turn, until now, it has been grown diamond wafer up to 5 mm diameter, only with high costs [4, 5].

Table 1 – Properties and some applications of diamond

Properties	Parameter	Dimension	Value	Interpreting	Importance
Mechanical	Crystal Lattice Constant	Å	3.567	The highest atomic density	Extreme mechanical strength and stability as well as hardness against breaking erosion and wearing from solid surface contacts. A perfect material for micromechanics
	Crystal Lattice Energy	J/kmol	720	The strongest atomic bond	
	Hardness	Kg/mm ²	10 ⁴	The highest resistance against a penetration of external atoms in the lattice	
	Moh's Hardness	-	10		
	Compression	Pa ⁻¹	10 ⁻¹²		
Friction coefficient	-	7x10 ⁻² 1.4x10 ⁻¹	Low friction (wear resistant) material		
Thermal	Thermal conductivity	W/cmK	20	The Highest dissipated electrical power	The best heat-conducting material, keeping its size and mechanical properties up to the highest temperatures. A perfect material for substrates of integrated elements and for vacuum cathodes
	Thermal expansion	°C ⁻¹	1.1x10 ⁻⁶	The lowest changing of overall dimension, varying the temperature	
	Melting point	°C	4x10 ³	Mechanical stability up to highest temperatures	
Magnetic	Magnetic susceptibility	Cm ³ /g	-4.9x10 ⁻⁷	Low value	Diamagnetic material
Optical	Transparency	%	98	The most transparent material in the visible range	A good material for waveguides, electron optic switches, photon windows, high power lasers and other photon components, including displays
	Absorption edge	µm	0.2	Small value	
	Refractive index (synthetic diamond)	-	2.465 at λ=400nm	High value	
Radiation	Non-sensitive material up to radiation energy of 5.45 eV			Radiation hard material	sensors, using intrinsic diamond
Chemical	Fully inert material against acids and alkalies (except in the presence of oxidant)			Chemically inert material	Independent operation of the environment, including corodent and biomedica

Table 2 – Electrical parameters of wide bandgap semiconductors

	IMPACT	SI	GAAS	4H SIC	GAN	DIAMOND	UNITS
Bandgap Energy	P _{out} (V _{max})	1,1	1,47	3,26	3.5	5.45	eV
Max. Electric Field	P _{out} (V _{max})	0.41	0,48	3	5	10	MV/cm
Electron Mobility	R, f _{ts} P _{out} (I _{max})	1450	8600	900	2000	4500	cm ² /Vs
Hole Mobility	R, f _{ts} P _{out} (I _{max})	480	130	120	200	3800	cm ² /Vs
Saturation Velocity	f _t	0.86	0.72	2	2.5	2.7	10 ⁷ cm/s
Thermal Conductivity	P _{out} (T), f _t (T)	1.5	0.46	5	1.3	20	W/cmK
Substrate Diameter	Cost	300	150	75	75	5	mm

Considered for a long time one of the power technologies of the future, SiC may finally enter the mainstream. Silicon carbide exhibits a two-dimensional polymorphism called polytypism. All polytypes have a hexagonal frame of SiC bilayers. The hexagonal frame should be viewed as sheets of spheres of the same radius and the radii touching, as illustrated in [1]. The sheets are the same for all lattice planes. However, the

relative position of the plane directly above or below are shifted somewhat to fit in the “valleys” of the adjacent sheet in a close-packed arrangement. Hence, there are two unequivalent positions for the adjacent sheets [1].

If the first double layer is called the A position, the next layer that can be placed according to a closed packed structure will be placed on the B position or the C position (Fig. 1). The different polytypes will be constructed by permutations of these three positions. Thus, the only cubic polytype in SiC is 3C-SiC, which has the stacking sequence ABCABC... [1]. The two important polytypes already intensely used for power devices, 6H-SiC and 4H-SiC [1-3, 6-10], have stacking sequences ABCACBABCACB... and ABCBABCB... (Fig. 2), respectively. The number thus denotes the periodicity and the letter the resulting structure which in this case is hexagonal. All polytypes are SiC of equal proportions of silicon and carbon atoms, but due to the fact that the stacking sequence between the planes differs, the electronic and optical properties differ. The bandgap is, for instance, 2.39 eV for 3C-SiC, 3.02 eV for 6H-SiC, and 3.26 eV for 4H-SiC [1].

There are some 200 polytypes proven in existence, some with a stacking period of several hundred double layers [1]. It is hard to understand how these crystals grow since there has to exist some 'memory' which guides the atoms into the right stacking sequence. When for instance the 6H-SiC polytype grows each atom landing on the surface must sense at least 6 layers down in order to find its proper site.

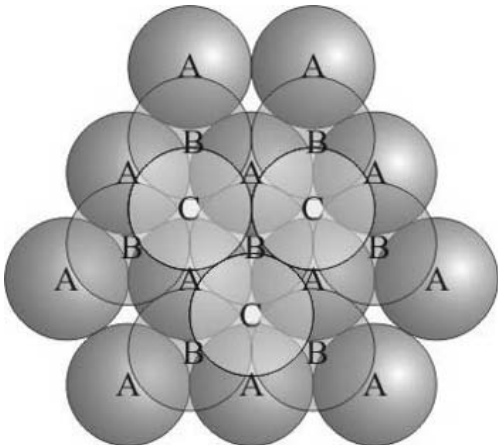


Fig. 1 – Illustration of three close-packed planes of spheres. The resulting structure in this example is 3C-SiC [1].

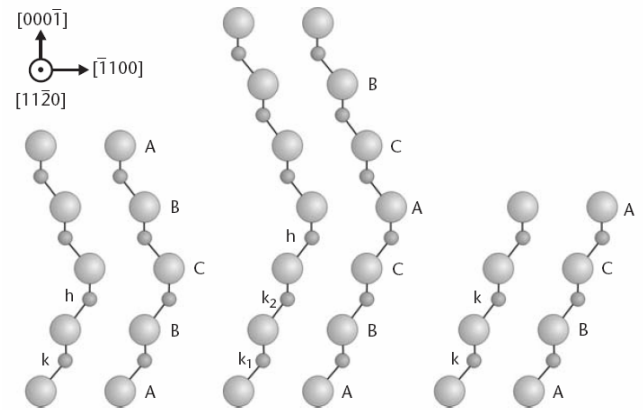


Fig. 2 – The three most common polytypes in SiC viewed in the [1120] plane. From left to right, 4H-SiC, 6H-SiC, and 3C-SiC; k and h denote crystal symmetry points that are cubic and hexagonal, respectively [1].

Over the last two decades, significant advances in the growth, doping, and processing technologies of SiC and diamond materials have been accomplished [1-10], triggering hopes for their use in high power electronics. With high-quality SiC crystals now available [1], the main challenge is the optimization of devices structures, in order to fully exploit the excellent material properties [1-3], [6-15]. With high-quality SiC crystals now available [1], the main challenge is the optimization of devices structures, in order to fully exploit the excellent material properties [1-3], [6-15]. Synthetic diamond has been produced with high-pressure, high-temperature technology and more recently by chemical vapor deposition (CVD). CVD offers a process for producing high-crystalline quality diamond under tightly controlled conditions.

The biggest problem of diamond remains the nearly total absence of shallow dopants [4-5]. Like for many wide band gap semiconductors, all known dopants in diamond are actually deep in the sense that their ionization energies are much higher than the room temperature thermal energy. However, due to its atomic density (the highest of any terrestrial material), diamond cannot easily incorporate other atoms into its crystalline structure. Boron is the only relevant known dopant for diamond, having activation energy of 0.37eV. The *n*-type dopant with the lowest activation energy is phosphorus (0.52eV). This value is still too high to expect a reasonable ionization rate. Therefore, only unipolar diamond devices, like *p*-type SBDs, are theoretically capable of high performances at room temperature.

3. IDEAL SBDs STRUCTURE. DESIGN RULES

The basic structure of the ideal SBD is presented in Fig. 3. A Schottky metal is deposited on an optimally designed epitaxial (drift) layer. The doping (N_e) and the thickness (t_e) of the epitaxial layer determine the specific on-resistance and blocking voltage capability of the diode. For a normal Schottky diode, (Fig. 3a), the depletion layer width (y_d) at breakdown is smaller than the drift thickness. This situation corresponds to a non punch through (nPT) structure and an ideal avalanche breakdown, respectively. A wide drift layer is required in order to obtain devices with high breakdown voltage. However, when forward biased, much of the drift region remains undepleted and increases the on-state resistance. To reduce this effect, the diode is often designed to ensure that this epitaxial zone is fully depleted before the breakdown occurs. The electrical field of such punch-through (PT) diode (Fig. 3b) is compared to that of the normal structure (nPT). The maximum electric field (E_M) and the slope of the field vs. distance in drift region (Fig. 3c) are the same for both structures at a given drift doping (see Fig. 3c and Fig. 4) [15-16].

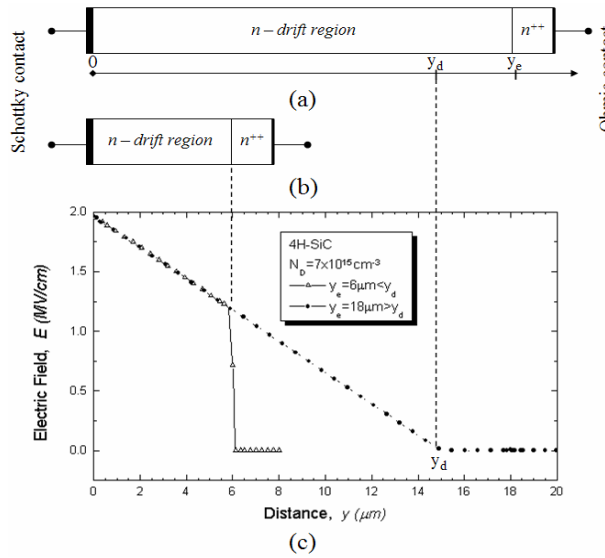


Fig. 3 – Ideal structures of: (a) nPT SBD; (b) PT SBD and (c)-simulated electric field distribution for both ideal structures (n⁺⁺ is substrate region)

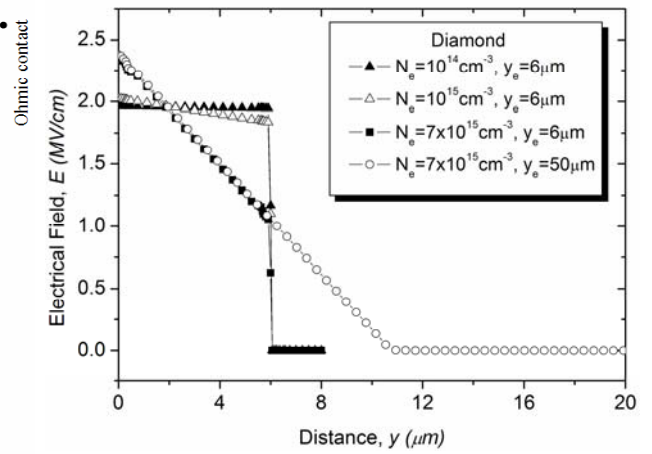


Fig. 4 – Electric field distribution in the drift region at breakdown for SBDs on diamond

The breakdown voltage is numerically equal with the area under the field vs. distance curve (Fig. 4) [15]. For nPT SBD is obtained:

$$V_{BR} = V_{BR,i} = \frac{qN_e}{2\epsilon} y_d^2, \quad (1)$$

while for PT diode results [15-16]:

$$V_{BR} = E_M y_e \left(1 - \frac{y_e}{2y_d} \right) \quad (2)$$

The maximum of the electric field at breakdown is given by [15]:

$$E_M = \frac{qN_e}{\epsilon} \cdot y_d \quad (3)$$

Thus, V_{BR} of PT diode is always less than of the normal structures. In Fig. 5, the variation of the breakdown voltage with the drift doping for ideal nPT and PT Schottky structures is shown. This dependence has a comparable slope for the diamond and SiC nPT diodes (Fig. 5a). In order to obtain an analytical

solution for these variations, a power law was used to fit the simulated data. The equations obtained and inserted in the legend of Fig. 5a are:

$$V_{BR} = 5 \cdot 10^{15} N_e^{-0.795} \quad \text{for SiC,} \quad (4)$$

$$V_{BR} = 3.4 \cdot 10^{15} N_e^{-0.781} \quad \text{for diamond.} \quad (5)$$

These expressions can be used to achieve the drift doping and the minimum drift thickness required for a given breakdown voltage.

In Fig. 5b the dependence of the breakdown voltage on the epi-layer doping on diamond and SiC, for PT SBDs, are presented. The V_{BR} decreases with doping for $N_e > 10^{15} \text{ cm}^{-3}$. For low drift dopings, the breakdown voltage is nearly constant for both diamond and SiC structures. These constant values can be explained based on the electrical field distribution in the epitaxial region shown in Fig. 4. At low drift dopings, the depletion width is very large ($y_d \gg y_e$) and expression (2) becomes:

$$V_{BR} \cong E_M y_e \quad (6)$$

Since the maximum electrical field has almost the same value at breakdown for any low doping (Fig. 4), the breakdown voltage is constant for $N_d < 10^{15} \text{ cm}^{-3}$. The difference between in V_{BR} obtained for PT SBD on diamond and 6H-SiC at low impurities concentrations (Fig. 5b) is due to the difference in field peak:

$$\frac{V_{BR,dia}}{V_{BR,SiC}} = \frac{E_{M,dia}}{E_{M,SiC}} \cong 1,18 \quad (7)$$

Another interesting result is that the breakdown voltage is not influenced by the drift region doping type. The same V_{BR} values were obtained for n -type and p -type doped epi-layers (Fig. 5b).

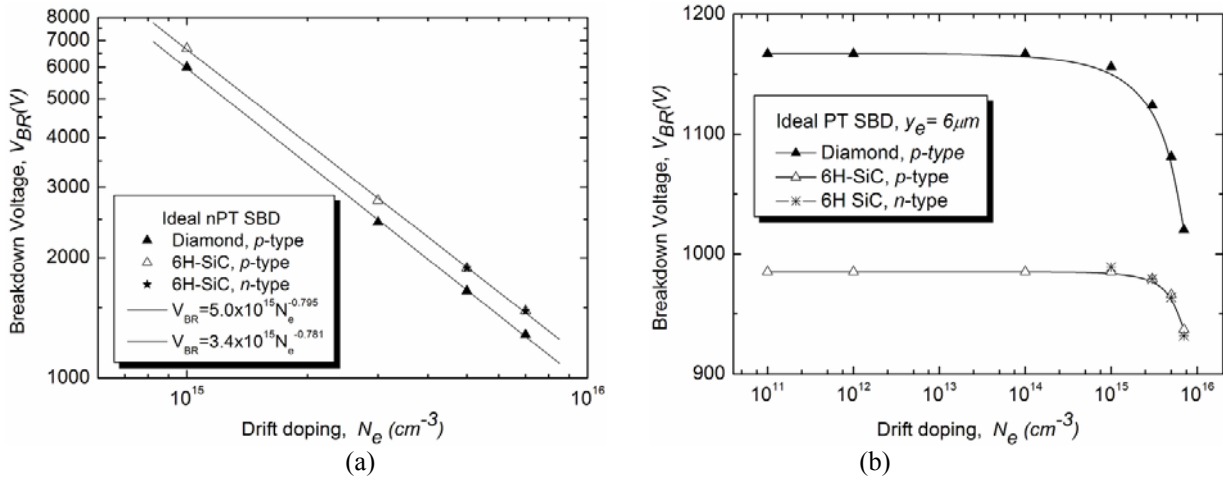


Fig. 5 – Breakdown voltage versus drift doping for ideal: a) nPT SBD and b) PT SBD.

The device specific on-resistance is a function of the epi-layer and substrate parameters (neglecting the ohmic contact resistance) [15]:

$$R_{on} \cong R_e + R_s \cong \frac{y_e}{q N_e \mu_n} + \frac{y_s}{q N_s \mu_{n,s}}, \quad (8)$$

where μ_n and $\mu_{n,s}$ are electron mobilities in drift and substrate epilayers, respectively.

Using equations (1-5), (8), the values of drift region doping and thickness can be calculated to determine the lowest specific on-resistance for a given breakdown voltage.

The design begins by choosing the epi-layer doping [15-16]. A high N_e is selected in order to achieve a large current capability. For example, with a doping of $1.1 \times 10^{16} \text{ cm}^{-3}$, a depletion layer of $10 \mu\text{m}$ is obtained by

simulations for a nPT SBD. For $y_d=y_e=10\mu\text{m}$, $R_{on}=0.91\text{ m}\Omega/\text{cm}^2$, corresponding to an ohmic drop smaller than $1V$ for high current density ($1000\text{A}/\text{cm}^2$). $V_{BR}=1\text{kV}$ was calculated for the above mentioned drift layer parameters, using eq. (1).

The forward voltage drop can be reduced by shortening the drift width (PT structure). In Table 3 are given values of V_{BR} and R_{on} calculated for a PT SBD at different epi-layer widths. A relative current gain (ΔR_{on}) and a decrease in blocking voltage (ΔV_{BR}) are obtained, when y_e is reduced.

Low epi-layer doping is required for high breakdown voltage. For a doping of $5.5\cdot 10^{14}\text{ cm}^{-3}$, simulations predict $V_{BR}=10730\text{V}$ and $y_d=145\mu\text{m}$ for nPT SBD (Table 3). If the drift layer is shorter ($y_e=100\mu\text{m}$), V_{BR} drops to 10kV (6.8% loss of off-state performance, only) and R_{on} decreases dramatically from $145\text{m}\Omega/\text{cm}^2$ to $126\text{m}\Omega/\text{cm}^2$ (30% improvement of the current capability). A voltage drop of 1.26V is calculated for a current density of $10\text{A}/\text{cm}^2$.

Some alternative designs of PT SBD with this low drift doping are also presented in Table 3.

From the table data one may deduce that the optimum design corresponds to a slightly punch-through structure for high epi-layer dopings and to a deep PT for low concentration. For drift widths below the ones in Table 3 the current gain becomes smaller than the loss in blocking capability.

Table 3 – Alternate designs for 4HSiC PT-SBD [15]

N_e (cm^{-3})	y_e (μm)	R_{on} $\text{m}\Omega/\text{cm}^2$	ΔR_{on} (%)	V_{BR} (V)	ΔV_{BR} (%)
$1.1\cdot 10^{16}$	10	0.910	-	1000	-
$1.1\cdot 10^{16}$	8	0.771	15	960	4
$1.1\cdot 10^{16}$	6	0.618	32	840	16
$1.1\cdot 10^{16}$	4	0.464	49	640	36
$1.1\cdot 10^{16}$	2	0.310	66	360	64
$5.5\cdot 10^{14}$	145	179	-	10730	-
$5.5\cdot 10^{14}$	102	126	30	10000	6.8
$5.5\cdot 10^{14}$	80	99	45	8519	20.6
$5.5\cdot 10^{14}$	50	62	65	6075	43

4. OXIDE RAMP TERMINATION

In real devices, the breakdown voltage is always less than that predicted by theory, since the material is not perfect (crystal defects) and the electric field is crowding at the electrode corner [1].

These high fields can be relieved by using edge termination surrounding the electrode periphery [8-12, 14, 17-19]. An effective edge termination makes the electric field distribution uniform in the bulk and at the electrode corner and take the breakdown capability of the device closer to its theoretical limit. There is a variety of possible termination structures: guard rings [8, 9], field plates [8, 10, 11, and 12], mesa structures [8], high resistivity layers, junction termination extensions [8, 10] or some combinations of techniques [6-8]. Many of these edge terminations are involved with pn junctions: guard ring, junction termination extensions.

The field plate technique is probably the simplest for edge termination. The field plate consists of a metal overlapping an oxide layer that provides field relief and smoothes the field lines at the contact periphery [10-12]. In Fig. 6a is shown a single step field plate structure, obtained by etching the oxide layer deposited on the drift layer [17]. The termination has two parameters: the thickness of the oxide (t_{OX}) and the length of the field plate (FP). A more accurate solution, three-step field plate structure, presented in Fig. 6b, complicates the fabrication process but enhances the device's electrical performance [17], which itself can be adjusted by varying six parameters: the thicknesses of the three oxide ramps (T_{F1} , T_{F2} and T_{F3}), the lengths of ramps 1 and 2 (X_{F1} and X_{F2}) and the length of the field plate on top of the oxide (FP), (see Fig. 6b).

We had previously patented a effective field plate edge technique that offers nearly ideal plane parallel breakdown [11-14]. The termination, shown in Fig. 6c which was successfully tested on Si, SiC and diamond power devices [11-14, 17-18] is based on a field plate overlapping on oxide ramp at the periphery of the Schottky contact. This oxide ramp termination is acknowledged by the international community as a highly efficient termination for power devices [8, 10].

Since n -type regions are nearly impossible to be obtained in diamond and, since many edge terminations concepts are based on pn junctions, the field plate concept is recommended to be used for terminating diamond devices [17-18].

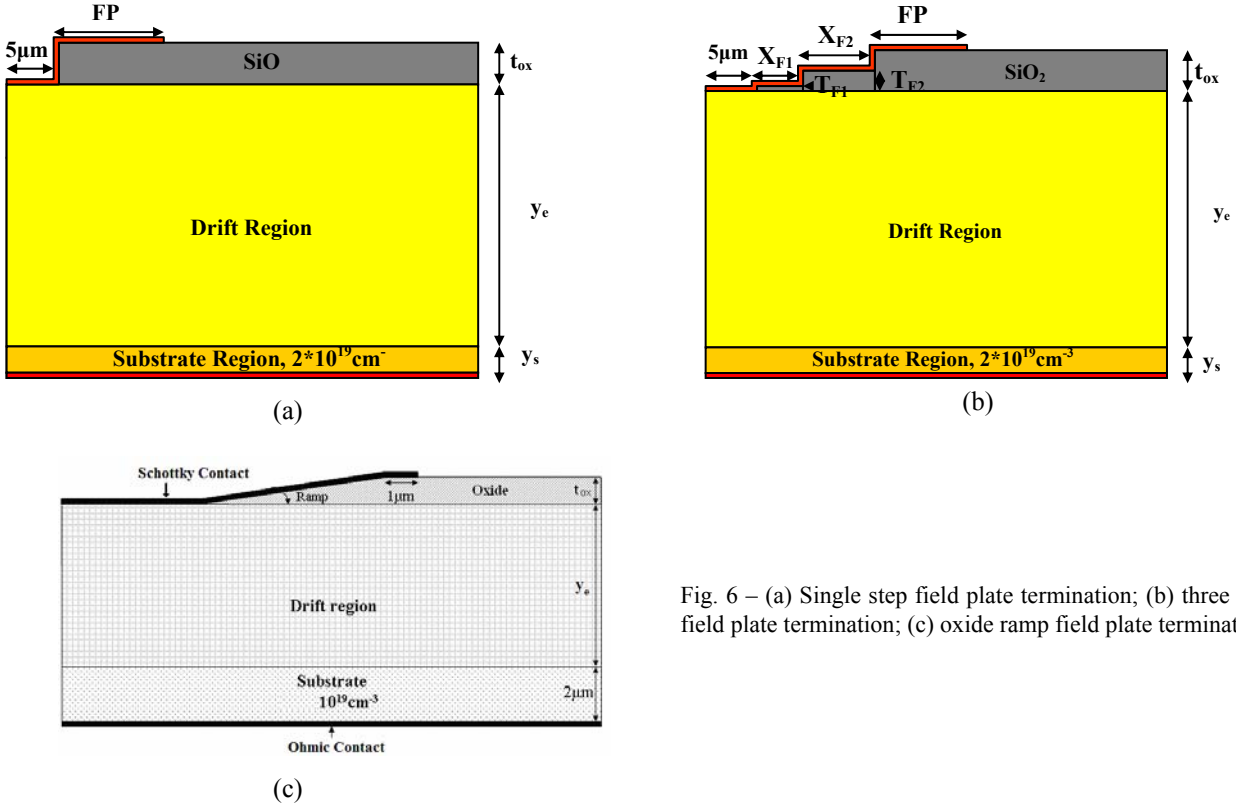


Fig. 6 – (a) Single step field plate termination; (b) three step field plate termination; (c) oxide ramp field plate termination

The performance of a termination is assessed by comparing the breakdown voltage of the ideal structure with that of the terminated structure. For ideal SBDs, the breakdown voltage is equal to the bulk breakdown, while in real devices V_{BR} is always lower due to edge effects.

Hence, we can define the termination efficiency (η) as the ratio between the simulated breakdown voltage of the SBD with a termination and the breakdown voltage of the ideal SBD structure [17-18]. The variation of the efficiency with the termination parameters, for SBDs with different field plate terminations is shown in Figs. 7 and 8. In the cases of single and three steps field plate diamond structures η increase at low values of the length of the field plate whilst for larger FPs, the breakdown voltage reaches its best performance (Fig. 7).

The potential distribution can be even more refined when using the ramp oxide termination which can be considered an infinite-step field plate structure [17-18]. The angle effect of the oxide ramp field plate structure is shown in Fig. 8 for PT and nPT SBDs based on SiC and diamond, respectively. The efficiency decreases with the ramp angle. The influence of the oxide thickness on the termination performance is illustrated in Fig. 9. The breakdown voltage increases with the oxide thickness and saturates at $2.5\mu\text{m}$ for both diamond and SiC SBDs.

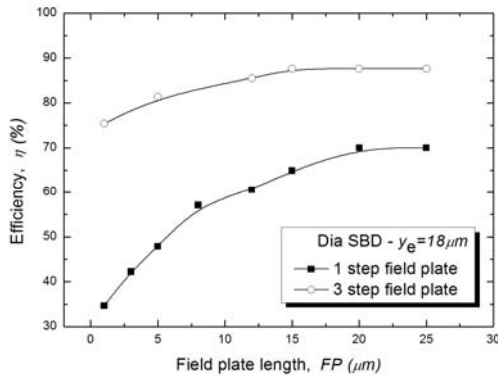


Fig. 7 – Termination efficiency vs. field plate length for single step and three step terminations

Hence, the termination efficiency is high and practically independent of semiconductor used at low ramp angles and thick oxide layers (Figs. 8 and 9). For the ranges of ramp angles and oxide thicknesses taken into consideration, the PT structures exhibited larger efficiencies than the nPT ones (Fig. 8).

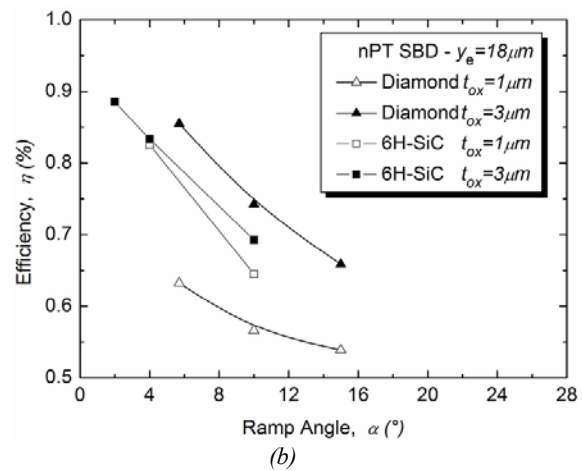
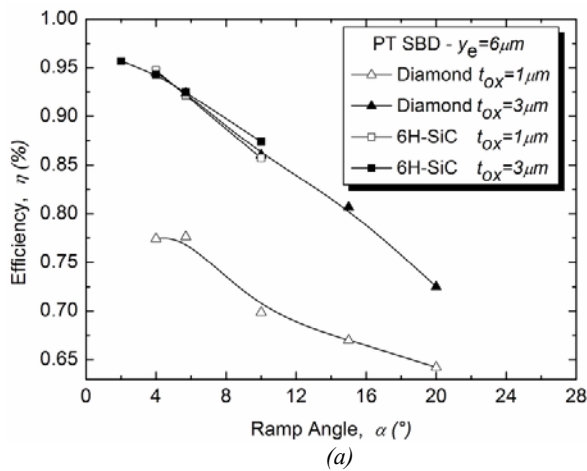


Fig. 8 – The dependence of the efficiency on the ramp angle for: a) PT SBD and b) nPT SBD.

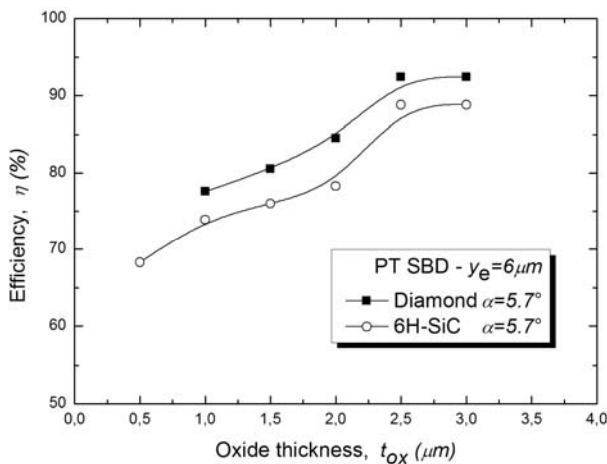
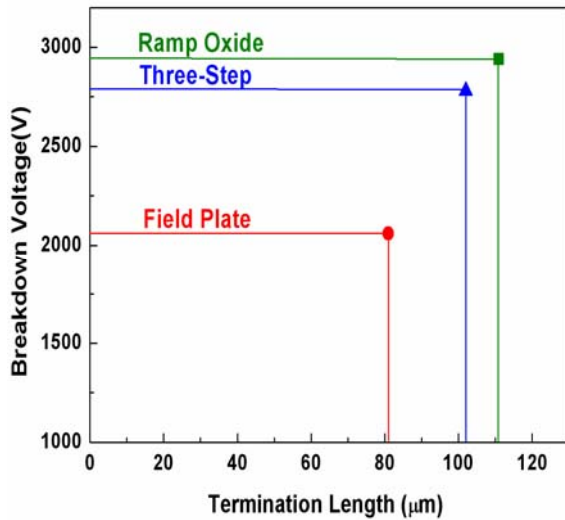


Fig. 9 – Efficiency vs. oxide thickness for oxide ramp termination

When performing the optimization of a termination structure, apart from maximizing the breakdown capability, the area consumption issue also needs to be addressed [17]. This comes to finding the optimum potential distribution within certain limited space. A termination with outstanding electronic parameters which occupies a large area may not be the optimum solution. A comparison of the area required by the best structure of each of the three terminations is included in Fig. 10. Although it has the worst electrical performance, the single step field plate termination requires an area 20% smaller than the three-step and ramp oxide structures, which exhibit termination efficiencies 25% and 30%, respectively, higher. Occupying

nearly the same area and having slightly better off-state performance than the three-step field plate, the ramp oxide appears to be the best choice for terminating diamond Schottky diodes [17]. Issues such as the complexity and cost of the fabrication process also have to be taken into consideration for fully comparing the merits of each structure.

Dependence of the termination efficiency on drift thickness is shown in Fig.11. A 10% - 20% decrease of the electrical capability of each termination can be noticed. By increasing of the drift thickness, the surface electric field stress at the edge of each termination is larger. Therefore, semiconductor's critical electric field value and, by consequence, the avalanche breakdown, are reached for smaller voltages [17].



Structure	$V_{BR}/\text{Termination Length}$
Single Step	25 V/μm
Three Step	27 V/μm
Ramp Oxide	26 V/μm

(a)

(b)

Fig. 10 – (a) breakdown voltage vs termination length; (b) comparable area consumption for each of the field plate terminations

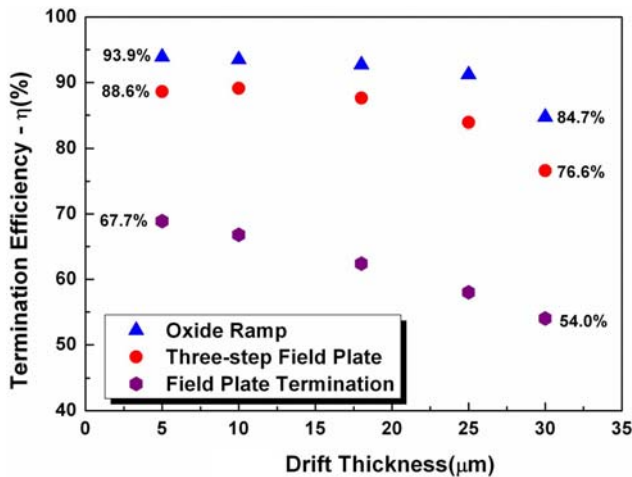


Fig. 11 – Variation of the terminations efficiency with the drift thickness for the three structures investigated

4. SBDs FABRICATED ON SIC AND DIAMOND

Table 4 presents the history in the main parameters of the silicon carbide and diamond devices produced in Romania. Three kinds of SiC diodes and one SBDs on diamond have been designed, fabricated and characterized in our country. The best performances of these devices are listed in Table 4.

High voltage SBDs have been obtained based on oxide ramp field plate termination [13-14, 17-19]. SiC Schottky structures were realized on different nm^+ 6H and 4H-SiC wafers. The n epi-layer has 8μm thickness and $8.5 \times 10^{15} \text{cm}^{-3}$ doping, or 5μm/ $2.7 \times 10^{16} \text{cm}^{-3}$ [13-14].

The main technological challenge of the targeted silicon carbide diode is fabrication of an efficiency oxide ramp termination. In order to obtain different oxide ramp angles various combinations of oxide layers have

been deposited on test samples. The wet etching process have been also studied using the standard oxide etch solution and a specific solution containing flouridic and nitric acids diluted in a large proportion of water [13, 14].

Table 4 – SiC and Diamond devices produced in Romania

Fabrication year	1997	2001	2002	2005
Device	<i>pn</i> diodes on 6H-SiC	Schottky diodes on 4H-SiC	Photodetectors on 6H-SiC	Schottky diodes on diamond
Current capability	> 10A	> 1A	> 100mA/W	> 1A
Blocking voltage	> 400V	> 1100V	> 200V	> 1200V

Two insulating layers comprised of an undoped oxide layer and an 8% phosphorus doped oxide layer were grown onto the epilayer. Then two steps wet etching were used: an initial etching in a standard oxide etch solution, followed by an over-etching in a P-etch solution. Experimental measurements indicate that an oxide ramp termination with an angle smaller than 4° was achieved. After oxidation, nickel (Ni) e-gun evaporation is performed on the heavily doped backside substrate and annealed at 1000°C to obtain a good ohmic contact. 1500\AA Ni was deposited and patterned by lift-off as Schottky contact on SBD. A high vacuum annealing at three temperatures ($800, 900, 1000^\circ\text{C}$) for 2min, was performed to form Ni Schottky barrier contact [13-14].

Fig. 12 shows the high efficiency of the oxide ramp termination in spreading the potential lines in the proximity of the Schottky contact. One can see that punch-through junction limits the breakdown voltage. Electric field lines are also shown as dashed lines [14].

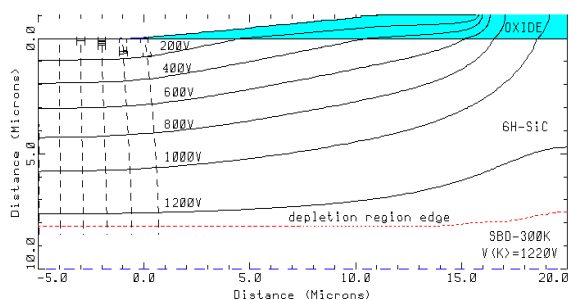


Fig. 12 – The potential distribution at breakdown voltage in SBDs with $8\mu\text{m}/8.5 \times 10^{16}\text{cm}^{-3}$ epilayer parameters.

Figs. 13-14 show current - voltage characteristics measured on SiC SBDs metalized with Ni. The Schottky contact annealing effect is evinced. Reverse leakage current increases with the increase in the reverse bias for unannealing devices (Fig. 13). A significantly improved of the reverse characteristics is proved after the annealing. A sharp breakdown at a maximum value of 1070V ($800^\circ\text{C}/2\text{min}$ annealing) can be observed [13]. Note that the breakdown voltage measured on Ni diodes represents 95% of the simulated corresponding value [13-14]. The reverse leakage current has a weak dependence on voltage for $V_R > 100\text{V}$.

The measured forward characteristics of Schottky barrier diode at different temperatures are shown in Fig. 14. The conduction mechanism follows the thermionic emission law for at least 6 orders of magnitude into low current density levels (Fig. 14).

The saturation current density (J_s), emission coefficient (n), Schottky barrier height (Φ_{Bn}) values extracted using an accurate parameter extraction software [13] are given in Table 5. The values of n do not vary with temperature (T), evincing a high quality Schottky contact.

The constant value of the Schottky barrier with temperature is expected since the bandgap of SiC barely changes within the investigated temperature range. The relatively large barrier of Ni on SiC allows operation of the Schottky diodes at high temperatures with lower power losses compared to equivalent structures using metals such as Ti, which have smaller barrier height to SiC [14]. The above mentioned V_{BR} of 1070V (Fig. 13) is roughly 10X lower than the highest reported V_{BR} [3], but with 5x smaller R_{on} (Fig. 14).

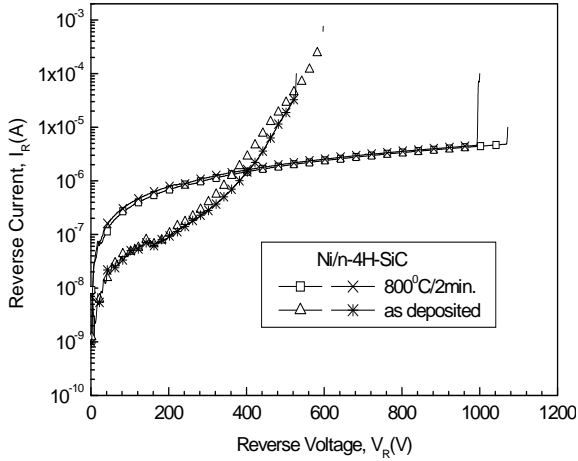


Fig. 13 – Reverse characteristics measured on Ni/n 4H-SiC Schottky Barrier Diodes

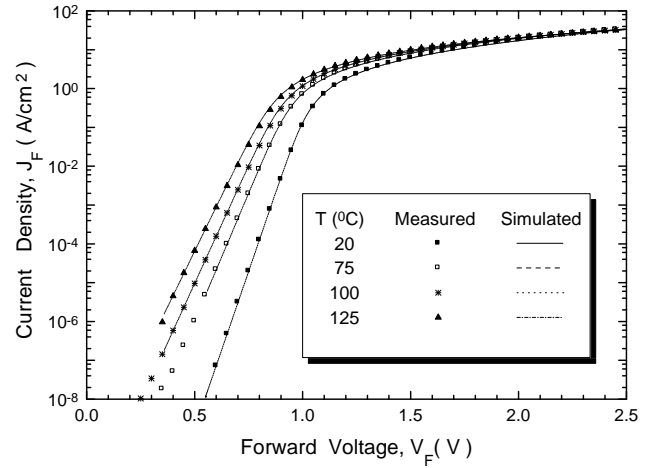


Fig. 14 – Calculated and measured forward current density vs. voltage for different temperatures on Ni/n 4H-SiC SBD.

Table 5 – Extracted Schottky parameters of SBD at various temperatures

T[°C]	20	75	100	125
J_s [A/cm ²]	1.6×10^{-17}	2.7×10^{-13}	7.9×10^{-12}	1.3×10^{-10}
Φ_{Bn} [V]	1.375	1.369	1.363	1.363
n	1.07	1.10	1.11	1.11

High voltage Schottky devices with oxide ramp termination were also fabricated on pp^+ diamond probes. In order to achieve the low angles required for optimum electrical behavior, three oxide layers were deposited on the intrinsic diamond [17]. After the low pressure chemical vapour deposition (LPCVD) of an undoped, $0.8\mu\text{m}$ thick, SiO_2 layer, two doped oxide layers were added, each of them $0.7\mu\text{m}$ thick, the first having 10^{12} cm^{-3} phosphorus concentration and the second $5 \times 10^{13}\text{ cm}^{-3}$. The etching rate of undoped SiO_2 is lower than that of phosphorus-doped SiO_2 . When immersed in a P-etch solution, the three oxide layers etch at different speeds, and thus the ramp oxide is obtained. After the deposition of gold, a structure with $\alpha=11^\circ$, $t_{OX}=2.2\mu\text{m}$ and $FP=1\mu\text{m}$ was obtained as illustrated in Fig. 15.

As shown in Fig. 16, which presents an experimental reverse curve, the measured breakdown voltage was approximately 1100V for a nominal drift thickness of $13\mu\text{m}$ and a circular Schottky contact with $40\mu\text{m}$ diameter (Fig. 15). However, when trying to match with the simulations, a comparable V_{BR} was obtained for $y_e=7\mu\text{m}$ as highlighted in Fig. 17 [17]. This discrepancy may be due to the high tolerance with which y_e was measured, to defects which might have appeared during the diamond growth or to the fact that the simulator implementation of diamond needs further refinement [17]. Reliable ionization coefficients for diamond still need to be determined. In the simulation carried out to fit the experimental results, the ionization coefficients used were obtained via extrapolation from silicon and silicon carbide, based on diamond's band gap. However, this did not yield accurate results [17].

In Fig.18 are shown forward characteristics measured on diamond SBD at three temperatures (300K , 400K and 507K) [19]. For low voltage the forward current increases with temperature. For larger V_F , the opposite trend can be noticed. In the first region, the current behaviour is dominated by the larger concentration of dopants which are ionized at elevated temperatures. Due to the higher ionization rate, more carriers are available for conduction and the current increases with temperature. As current rises, as shown before, the voltage drop across the internal resistances is dominant. This effect is related to the degradation of the mobility at high temperature due to various scattering mechanisms which occur in single crystal diamond.

In Fig.18 are shown forward characteristics measured on diamond SBD at three temperatures (300K , 400K and 507K) [19]. For low voltage the forward current increases with temperature. For larger V_F , the opposite trend can be noticed.

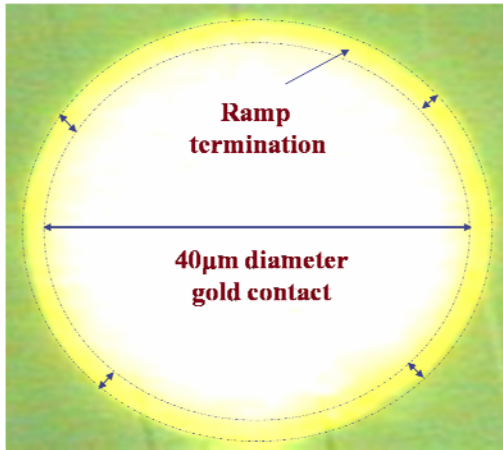


Fig. 15 – Diamond SBD with oxide ramp termination

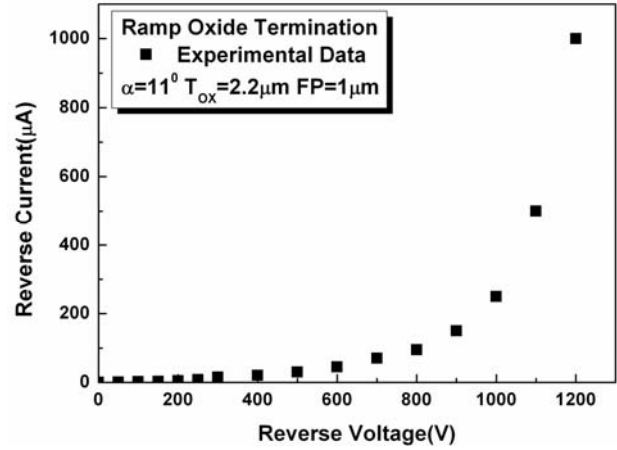


Fig. 16 – Reverse Characteristic Measured on Diamond SBDs.

In the first region, the current behavior is dominated by the larger concentration of dopants which are ionized at elevated temperatures. Due to the higher ionization rate, more carriers are available for conduction and the current increases with temperature. As current rises, as shown before, the voltage drop across the internal resistances is dominant. This effect is related to the degradation of the mobility at high temperature due to various scattering mechanisms which occur in single crystal diamond. Thus, the voltage drop increases with the temperature [19].

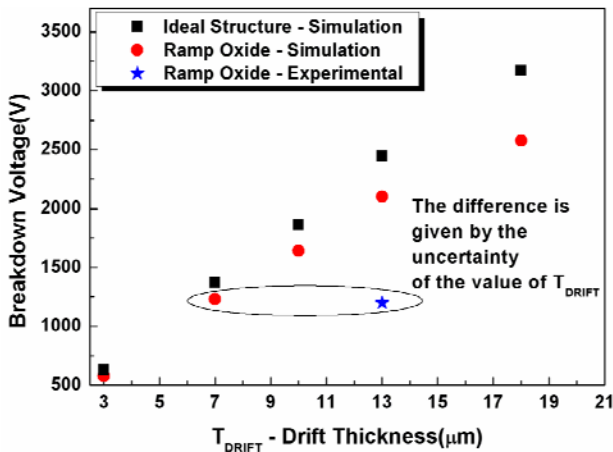


Fig. 17 – Breakdown voltage vs drift thickness for the ideal structure (simulation) and for the SBD with ramp oxide termination (simulation and experimental) [17].

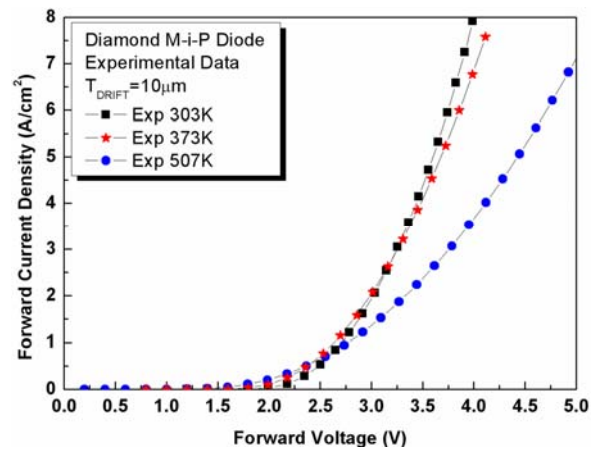


Fig. 18 – Measured on-state characteristics at different temperatures [19].

5. CONCLUSIONS

Diamond and SiC are materials expected to play a vital role in the new generation of power devices. The Schottky Barrier Diodes built on these semiconductors and presented in this paper prove their capability for high power and high voltage operation.

Punch-through and non punch-through structures were analyzed. For nPT SBDs, an analytical equation for the breakdown voltage vs. drift layer doping variation, often used in the power devices design, was achieved. It was shown that V_{BR} decreases with the drift doping with the same slope for both SiC and diamond SBDs. For PT structures, V_{BR} is constant at low epi-layer dopings and decreases for higher concentrations. Due to technological difficulties in doping diamond, extremely lowly doped drift layers, ideally intrinsic, are recommended for PT diamond SBDs. On the contrary, drift dopings around 10^{15} cm^{-3} are preferable for high power SiC SBDs, due to problems in growing lowly doped epi-layers. The low values

of the leakage currents calculated in both *n*-type and *p*-type SiC diodes, as well as in *p*-type diamond structures, enable the hope for the possible use of these devices in high temperature applications.

The trade-off between the current capability and the blocking potential corresponds to a slightly punch-through design, for large forward currents, and to a fully punched-through SBD at high breakdown voltage.

The performances of diamond and SiC Schottky barrier diodes terminated with three different structures, based on the field plate concept have been investigated. A simulation-based comparison between the three terminations, consisting of blocking ability and area consumption considerations, has been carried out. The efficiency of the single step field plate termination is 25% less than those of the other two structures, but it requires 20% less area. The ramp oxide termination, based on a field plate overlapping on oxide ramp at the periphery of the contact, exhibited the largest breakdown voltage with an area consumption comparable to that of the three-step field plate structure.

In this paper we demonstrated by measurements and simulation that the oxide ramp termination is highly suitable for SiC and diamond SBD. Values of the efficiency over 80% have been obtained for any ramp angle smaller than 12° and for oxide thicknesses over $2.5\mu\text{m}$ for diamond and SiC.

SBDs on SiC and Diamond have been fabricated for the first time in Romania using oxide ramp termination. The forward characteristics measured on SiC devices metalized with Ni, are in very good agreement with the thermionic emission theory at low level injection. An ideality factor close to one and a Schottky barrier unchanged with temperature up to 125°C were obtained. The experimental reverse characteristics of Ni/6H-SiC Schottky barrier diodes showed a near-ideal parallel plane breakdown at a voltage of 1070V and low leakage currents.

Results obtained from actual fabrication of diamond SBD with ramp oxide termination are also presented. Experimental results included in this paper have shown the capability of diamond Schottky structures of conducting on-state current densities up to 100 A/cm^2 at 5V . Two trends of variation were also experimentally revealed when considering the way the forward characteristic is influenced by the temperature. For forward voltages close to the turn-on voltage, the current increases with temperature. For larger V_F , an opposite dependence have been observed, because the series resistance effect becomes dominant.

A breakdown voltage over 110V has been measured on diamond diodes. The lack of simulation-experimental match indicates the need for further material investigation and for reliable determination of ionization coefficients for synthetic single crystal diamond.

5. REFERENCES

1. SADDOW, S., AGARVAL, A., Advances in Silicon Carbide Processing and Applications, Artech House, 2004.
2. SUGAVARA, Y., Recent Progress in Silicon Carbide Power Device Developments and Application Studies, in Proc of the 18th International Symposium on Power Semiconductor Devices and ICs (ISPSD), Cambridge, U.K., pp.10-18, 2003.
3. RUPP, R., TREU, M., VOSS, S., BJORK,F., REIMAN,T., 2nd Generation SiC Schottky diodes: A new Benchmark in SiC Device Ruggeness in Proc of the 18th International Symposium on Power Semiconductor Devices and ICs (ISPSD), Napoli, Italy., pp.269-273, 2006.
4. GURBUZ, Y., KANG, W.P., DAVIDSON, J.L., KERNS, Jr.,D.V., ZHOU, Q., PECVD diamond-based high performance power diodes", IEEE Transactions on Power Electronics, vol. 20 , pp. 1-10, 2005.
5. J. E. BUTLER, J.E., GEIS, M. W., KRON, K. E., LAWLESS Jr, J., DENEALT, S.,LYSZCZARZ, T. M., FLECHTNER, D., WRIGHT, R., Exceptionally high voltage Schottky diamond diodes and low boron doping , Semicond. Sci. Technol. 18, pp. S67-S71, 2003.
6. SINGH, K., COOPER, J.A., MELOCH, M.R., CHOW, T.P., PALMOUR, J.W., SiC Power Schottky and pin Diodes, IEEE Trans. El. Dev., vol. 49 , pp. 665-672, 2002.
7. RUPP, R., ZVEREV, I., SiC Power Devices: How to Be Competitive Towards Si-based Solutions, ECSCRM'02, published in Materials Science Forum, vols. 433-436 , pp.805-812, 2003.
8. TARPLEE, M.C., MADANGAGLY, V.P., ZHANG, Q., SURDARSAN, T.S., Design Rules for Field Pate Edge Termination in SiC Schottky Diodes, IEEE Trans. El. Dev., vol. 48, pp 2659-2664, 2001.
9. SHERIDAN, D.C., NIU, G., MERRETT, J.N., CRESLLER, J.D., ELLIS, C., TIN, C.C., Design and Fabrication of Planar Guard Ring Termination for High Voltage SiC Diodes, Solid St. Electron., vol. 44, pp1367-1372, 2000.
10. LA VIA, F. ROCCAFORTE, R., DI FRANCO, S. RAINIERI, V. MOSCATELLI, F. SCORZONI, A. CARDINALI, G.C., Comparison Between Different Schottky Diode Edge Termination Structures: Simulation and Experimental Results, ECSCRM'02, published in Materials Science Forum, vols. 433-436 pp.827-830, 2003.

11. BREZEANU, G., FERNANDEZ, J., MILLAN, J., BADILA, M., DILIMOT, G., MEDICI Simulation of 6H-SiC Oxide Ramp Profile Schottky Structure ICSCRM'97, Materials Science Forum, vols. **264-268**, pp.941-944, 1997.
12. BADILA, M., BREZEANU, G., MITU, F., Schottky Oxide Ramp Diodes in John Wiley Encyclopedia of Electrical and Electronics Engineering, John Wiley & Sons, Inc., New York, vol. 18, pp. 710-718, 1999.
13. BREZEANU, G., BADILA, M., TUDOR, B., MILLAN, J., GODIGNON, P., UDREA, F., AMARATUNGA, G.A.J., MIHAILA, A., Accurate Modelling and Parameter Extraction for 6H-SiC Schottky Barrier Diodes With Nearly Ideal Breakdown Voltage, IEEE Trans. El. Dev., vol. **48**, pp. 2148-2153, 2001.
14. BREZEANU, G., BADILA, M., UDREA, F., MILLAN, J., GODIGNON, P., MIHAILA, A., AMARATUNGA, G.A.J. BREZEANU, M., BOIANCEANU, C., High Performance SiC Diodes Based on an Efficient Planar Termination, in Proc of the 26th IEEE International Semiconductor Conference, Sinaia, Romania, pp.27-38, 2003.
15. BREZEANU, G., A short history. An analytical approach for SiC power devices, in Proc. of 28th IEEE International Semiconductor Conference, Sinaia, Romania, pp.345-348, 2005.
16. BREZEANU, G., VISOREANU, A., BREZEANU, M., UDREA, F., AMARATUNGA, G.A.J., ENACHE, I., RUSU, I., DRAGHICI, F., OFF- State performance of Ideal Schottky Barrier Diodes (SBD) on Diamond and Silicon Carbide, in Proc of the 29th IEEE International Semiconductor Conference, Sinaia, Romania, pp.319-322, 2006.
17. BREZEANU, M., AVRAM, M., RASHID, S.J., AMARATUNGA, G.A.J., BUTLER, T., RUPESINGHE, N.L., UDREA, F., TAJANI, A., DIXON, M., TWITCHEN, D.J., GARRAWAY, A., CHAMUND, D., TAYOR, P., BREZEANU, G., Termination Structures for Diamond Schottky Barrier Diodes, in Proc of the 18th International Symposium on Power Semiconductor Devices and ICs (ISPSD), Napoli, Italy, pp. 73-76, 2006.
18. BREZEANU, G., BREZEANU, M., UDREA, F., AMARATUNGA, G.A.J., BOIANCEANU, C., ZEKENTES, K., VISOREANU, A., Comparison between Schottky Diodes with Oxide Ramp Termination on Silicon Carbide and Diamond" in Proc. of 6th European Conference on Silicon Carbide and Related Materials (ECSCRM), Newcastle, UK, pp 24 (to be published in Material Science Forum), 2006.
19. BREZEANU, M., RASHID, S.J., AMARATUNGA, G.A.J., RUPESINGHE, N.L., BUTLER, T., UDREA, F., BREZEANU, G., On State Behaviour of Diamond M-i-P Structures, in Proc. of the 29th IEEE International Semiconductor Conference, Sinaia, Romania, pp. 311-314, 2006.

Received August 1, 2007